Modeling issues regarding thermal conductivity of graphene-based nanocomposites

Titus SANDU[*], Mihai GOLOGANU , Rodica VOICU , George BOLDEIU ,
and Victor MOAGAR-POLADIAN

[1]National Institute for Research and Development in Microtechnologies-IMT Bucharest,
126A Erou Iancu Nicolae, Bucharest,
[*]Corresponding author: titus.sandu@imt.ro

Abstract. Modeling thermal conductivity of graphene-based nanocomposites is analyzed from an effective medium approximation point of view, where interfacial thermal resistance and arbitrary shape of the fillers are considered. Two approximations, Maxwell-Garnett and coherent potential approximation, are used to show that the usual oblate spheroidal shape approximation of graphene nanodots is not satisfactory to model thermal conductivity in graphene-based composites.

Key-words: Composites, graphene, graphene-based composites, thermal conductivity, thermal interface materials, Maxwell-Garnett approximation, coherent potential approximation.

1. Introduction

Thermal conductivity and most notably the enhancement of thermal conductivity are major topics in thermal management applications of composite materials like the packaging and encapsulation of integrated circuits. Due to their good mechanical properties, polymers are chosen as matrix materials whilst metals or more recently carbon-based materials are preferred as fillers [1]. Nanocomposites or composites with nano-sized fillers are even more attractive for many thermal applications since their properties become dependent on the shape and on the size of the fillers [1–4]. This is true not only for the individual response of each nanoparticle filler [1, 2] but also thermal conductivities of the matrix and fillers are affected by the microscopic structure of the composite [3, 4]. While the thermal conductivity of metals spans the range of hundreds of W/m·K, carbon based materials like graphene and carbon nanotubes exhibit a thermal conductivity exceeding 2000–3000 W/m·K [5, 6] that makes them attractive for thermal interface materials [6, 7]. Thus polymers like epoxy may become candidates for such applications [6–8].

Beside their fabrication, composites and nanocomposites need models that satisfactorily predict and describe the effective properties like thermal conductivity or any other transport coefficient (*i.e.* electric conductivity, dielectric constant, etc.). Since the atomistic models are currently out of reach for many practical applications of composites and nanocomposites, the majority of models is based on continuum theories. For thermal applications continuum models assume constant conductivity in each component of the composite materials and calculate the effective thermal conductivity of the composite by solving the Laplace equation in heterogeneous media, which generates an averaged or homogenized response [9]. Moreover, modeling composites with finite element methods is useful in evaluating the strength of local fields but it may become sometimes prohibitive when high levels of accuracy are required [10,11]. The oldest approach is due to Maxwell-Garnett that is an effective theory for a particulate composite where each particle "feels" the field of the other particles like a polarization field induced in a large homogeneous sphere surrounding the particle [12]. In effective theories there is a given recipe by which the composite is "homogenized" often leading to bounds of the effective properties [2, 9]. For instance, it is known the formal analogy between the resolution of Laplace equation in heterogeneous disordered media and the resolution of the Schrödinger equation in disordered alloys [2]. Various approximations in the treatment of electronic structure in alloys are also used in the theory of effective thermal conductivity of composites: the averaged *t*-matrix approximation in electronic structure calculations [2, 13–15] is just the *Maxwell-Garnett Approximation* (MGA) [12], while the coherent potential approximation of electronic structures of alloys [2, 13, 16] has its correspondence in a *Coherent Potential Approximation* (CPA) regarding thermal conductivity of composites [2, 17].

In applications quite often shape approximations are made in order to model composites. Since ellipsoidal shapes can approximate many real situations and since the Eshelby's result [18], which states that, when subjected to a uniform excitation, the field inside of an ellipsoidal inclusion is itself uniform, a consistent theory of heat conduction in composites was established [19]. The connection of MGA with averaged *t*-matrix approximation was also proven [2, 17] such that compact formulae for ellipsoidal shapes were carried out [20]. These models consider thermal interface resistance as very thin shells around particles. Moreover, recent experiments [7, 21] have successfully used the MGA for shelled spheroids developed by Nan and coworkers in [20], where carbon nanotubes are modeled as very long prolate spheroids and graphene flakes as very thin oblate spheroids. [2, 20]. In this work, based on our previous results concerning both the dielectric behavior of biological cells [22] and the description of localized surface plasmon resonances in metallic nanoparticles [23-25], we extend and analyze the MGA and CPA models to calculate the effective thermal conductivities of composites having fillers of arbitrary shapes. By applying these methods to graphene-based nanocomposites we have found that the Nan's model of graphene flakes as thin oblates [20] cannot be applied to nanocomposites with graphene nanodots as fillers. Some preliminary results have been reported in a recent conference paper [26], here we provide additional details and we compare the effective thermal conductivities calculated with MGA and CPA models of graphene based nanocomposites. The paper has the following structure. The next section presents the MGA and the CPA models for fillers with arbitrary shape, followed by the sections presenting numerical results and the conclusions, respectively.

2. Maxwell-Garnett and coherent potential approximations of thermal conductivity in particulate composites with arbitrary shape fillers

The description of the problem regarding thermal conductivity in composites considers arbitrary distribution and arbitrary shapes of the particulate fillers dispersed in the matrix. The definition also considers a barrier resistance at the interface between matrix and particles. The composite can be thought of as a large representative volume V, eventually periodically replicated. The temperature field is designated by T and its gradient is proportional to the heat flux. The field temperature has basically two parts, the first $T^{0/0}$ is the fluctuating part and the second is the superimposed part which has a linear spatial dependence $\theta \cdot r$. Thus, the total temperature field is $T = T^{0/0} + \theta \cdot r$. The boundary conditions are set in such a manner that outside volume V the average gradient on the boundary is

$$\langle \nabla T \rangle = \int_{\partial V} (T^{0/0} + \theta \cdot r) n ds = \theta. \tag{1}$$

In equation (1) $\langle \rangle$ is the average, θ is the gradient that is proportional to the imposed heat flux, ∂V is the surface boundary of V and n is the normal unit vector to surface ∂V. The temperature field T obeys the Laplace equation

$$\Delta T(r) = 0 \tag{2}$$

inside each phase and the following boundary conditions

$$K_0 \frac{\partial T}{\partial n}\bigg|_+ = k_1 \frac{\partial T}{\partial n}\bigg|_- \tag{3}$$

$$\beta(T|_+ - T|_-) = K_1 \frac{\partial T}{\partial n}\bigg|_- \tag{4}$$

on each interface between the two phases. Equation (2) is just the heat equation in the steady-state in each phase, equation (3) is the continuity of the heat flux at the interface between matrix and particles, and equation (4) quantifies interfacial barrier resistance between matrix and particles. Thermal conductivities of the matrix and fillers are K_0 and K_1, respectively, and the thermal resistance at the interface between matrix and fillers is related to parameter β.

In composites there is a complete similarity between various transport phenomena, like electric, dielectric, thermal, etc. since they are described by the same governing equations. Therefore, a terminology proper to dielectric permittivity phenomena can be adopted and used thereafter. If a particle of volume V_1 is embedded in a uniform matrix and a uniform field/flux $\theta \cdot r$ is imposed across a macroscopic volume that includes the particle, the response of the particle is given as the normalized polarizability [22]

$$\alpha = \frac{1}{4\pi V_1} \int_{V_1} \frac{(k_1 - k_0)}{k_0} (-\nabla T(r)) d^3 r. \tag{5}$$

Equation (5) can be cast in the following form [22-25]

$$\alpha = \sum_k \frac{w_k(k_1 - k_0)}{k_0 + (1/2 - \chi_k)(K_1 - k_0)}, \tag{6}$$

where w_k is the coupling weight of the kth eigenvalue χ_k of an electrostatic operator defined on the boundary of V_1. Depending on the particle shape, w_k and χ_k are called shape factors. It can be straightforwardly checked that the normalized polarizability is in fact related to the t-matrix in the Nan's formulation [2, 17]. The numbers $1/2 - \chi_k$ are the generalization of the depolarization factors of those eigenmodes that can be excited by a uniform field (*i.e.* $w_k \neq 0$). For a general ellipsoid there are three eigenmodes that can be excited by uniform fields, one for each of the ellipsoid axis. Eshelby has shown that for uniform fields the field inside the ellipsoid is also uniform [18, 19] but this is not generally true for inclusions of arbitrary shapes. The Eshelby's result can be used in any homogenization scheme which is based on an effective medium approximation. In such schemes the local electric field E_L that is felt by a charge probe in the "homogenized" medium (the effective medium associated with the macroscopic composite) is of the form

$$E_L = E_0 + \frac{1}{k_0} \hat{S} \cdot P, \tag{7}$$

where E_0 is the applied field, P is the macroscopic polarization field and $\hat{S}$ is the Eshelby tensor that is diagonal with diagonal elements being just the depolarization factors $1/2 - \chi_k$ [19, 27]. Averaging Eq. (7) will lead to a Maxwell-Garnett formula for aligned but otherwise random mixture of ellipsoids [27]. For example, if the ellipsoids are aligned along *x*-axis the Maxwell Garnett formula is

$$k_{eff} = k_0 + fk_0 \frac{(k_1 - k_0)}{k_0 + (1/2 - \chi_k)(1 - f)(k_1 - k_0)}, \tag{8}$$

with f the volume concentration of the ellipsoidal fillers. Equation (8) can be rewritten as

$$k_{eff} = k_0 + fk_0 \frac{\langle \alpha \rangle_{or}}{1 - (1/2 - \chi_x)f\langle \alpha \rangle_{or}}, \tag{9}$$

where $\langle \alpha \rangle_{or} = \alpha_x = (k_1 - k_0) \Big/ \big(k_0 + (1/2 - \chi_x)(k_1 - k_0)\big)$ is the orientational averaging in this case.

The above result can be obtained also by a homogenization argument initially used by Maxwell-Garnett for spherical inclusions [12]. In a nutshell, one takes a macroscopic volume *V* of a composite of ellipsoidal shape with the same aspect ratios of its axes as those of the inclusions. It is supposed that the macroscopic ellipsoid has a conductivity that equals the effective conductivity of the composite k_{eff} and is embedded in a medium with conductivity k_0 of the matrix. The k_{eff} given by Maxwell-Garnett approximation is obtained by equating the polarizability of the macroscopic ellipsoid with the sum of the *N* individual polarizabilities of inclusions that can be found on average in the volume *V*. We extend this procedure to inclusions of arbitrary shapes. The scheme is presented in Fig. 1. First, the response of a single nanoparticle embedded in the matrix is calculated. Then by the Maxwell-Garnett approximation the effective conductivity is calculated either for aligned but otherwise randomly placed nanoparticles (the scheme depicted at the top of Fig. 1) or for both random positions and random orientations (the bottom of Fig. 1).
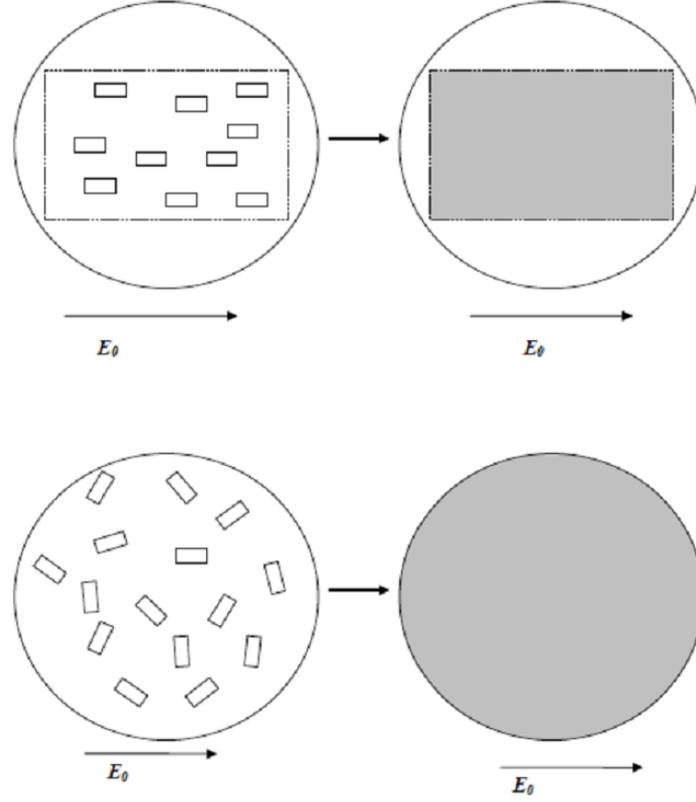
Fig. 1. Schematics of the homogenization procedure. The top of the figure shows the homogenization of aligned inclusions, while the bottom depicts the homogenization of randomly oriented inclusions.

Thus, for aligned inclusions the equation that gives the effective conductivity in the Maxwell-Garnett approximation for arbitrarily-shaped inclusions is

$$\sum_k \frac{w_k(k_{eff} - k_0)}{k_0 + (1/2 - \chi_k)(k_{eff} - k_0)} = f \sum_k \frac{w_k(k_1 - k_0)}{k_0 + (1/2 - \chi_k)(k_1 - k_0)}. \tag{10}$$

It is easily seen that Eq. (10) contains Eqs. (8) and (9) as particular cases.

For randomly oriented particles we use the procedure shown at the bottom of Fig. 1. The homogenization formula is

$$k_{eff} = k_0 \left(1 + \frac{f\langle\alpha\rangle_{or}}{1 - f\langle\alpha\rangle_{or}/3} \right), \tag{11}$$

where

$$\langle\alpha\rangle_{or} = \frac{\alpha x + \alpha_y + \alpha_z}{3}. \tag{12}$$

Generally, the term $f\langle\alpha\rangle_{or}$ is the averaged t-matrix [2, 17]. In a very dilute limit Eqs. (8), (9), (10) and (11) take a quite simple form

$$k_{eff} = k_0\big(1 + f\langle\alpha\rangle_{or}\big).\tag{13}$$

The local field effects are taken into account in Eq. (9) by the term $1/(1 - (1/2 - \chi_x)f\langle\alpha\rangle_{or})$ or the term $1/(1 - f\langle\alpha\rangle_{or}/3)$ in Eq. (11). In the case of Eq. (11) the term is just the Lorentz-Lorenz or Clausius-Mossotti approximation [27].

Since α is essentially the *t*-matrix in a scattering theory formulation another mean field approximation is the coherent potential approximation [2, 17]. In the coherent potential approximation, the effective conductivity of the composite k_{eff} is established by imposing the condition $\langle\alpha\rangle = 0$, which states that, in an effective medium background, any additional polarization given by a fluctuating inclusion is zero on average. The explicit form of the coherent potential approximation for arbitrarily-shaped inclusion is

$$\sum_k f\frac{w_k(k_1 - k_{eff})}{k_{eff} + (1/2 - \chi_k)(k_1 - k_{eff})} + (1 - f)\frac{w_k(k_0 - k_{eff})}{k_{eff} + (1/2 - \chi_k)(k_0 - k_{eff})} = 0.\tag{14}$$

Equation (14) just generalizes Bruggeman's formula [28] for spherical fillers and supposedly it is valid for higher volume concentration f than the MGA. The CPA model is more appropriate to study other phenomena like, for example, percolation, where the MGA cannot give reliable results due to the Clausius-Mossotti term [29].

The thermal contact resistance between matrix and filler can be modeled as a shell [20, 22]. Thus, the interfacial barrier resistance is given by a very thin shell of thermal conductivity k_2 [20]. We have shown in [22] that a shelled particle of arbitrary shape can be "homogenized" by replacing it with a particle that has an effective conductivity for each eigenmode:

$$k_{k\_eff} = k_2\left(1 + \frac{k_1 - k_2}{(1 + \eta)k_2 + \eta(1/2 - \chi_k)(k_1 - k_2)}\right).\tag{15}$$

Here η is a small parameter, such that $1 + \eta$ is the ratio between the outer and the inner volume of the shelled particle. The barrier resistance is obtained as the limit $\eta \to 0$ with $\eta/k_2 \to$ constant. Equation (15) is a just a generalization of the results given in [20]. We notice here that a thermal barrier provides an explicit dependence of effective conductivity on the size of the particles, which the Laplace equation does not provide only by itself [22-25].

3.   Thermal conductivity of graphene-based nanocomposites

In the following we have in mind as a benchmark a composite with graphene fillers and a generic polymer as a matrix. For calculations, a thermal contrast $k_1/k_0 = 1000$ is considered between graphene and the polymer. Exploiting the fact that spheroidal shapes have analytic expressions for the depolarization factors [30], graphene flakes are understood as very thin oblate spheroids in [5, 7, 21]. For an oblate spheroid with axes $a_x = a_y < a_z$ the asymptotic behavior of the depolarization factors are $1/2 - \chi_{x,y} \sim (a_z/a_x)^2$ and $1/2 - \chi_z \sim 1 - (a_z/a_x)^2$. Thus, for a thin oblate with an aspect ratio $a_z/a_x \le 1/1000$ a contrast $k_1/k_0 = 1000$ ensures the following depolarization factors $1/2 - \chi_{x,y} \approx 0, 1/2 - \chi_z \approx 1$. These conditions are fulfilled, for example, by micrometer-sized graphene inclusions.

In Fig. 2 we plotted the thermal enhancement factor k_{eff}/k_0 of a graphene-based composite as a function of volume concentration of filler in the Maxwell-Garnett approximation.
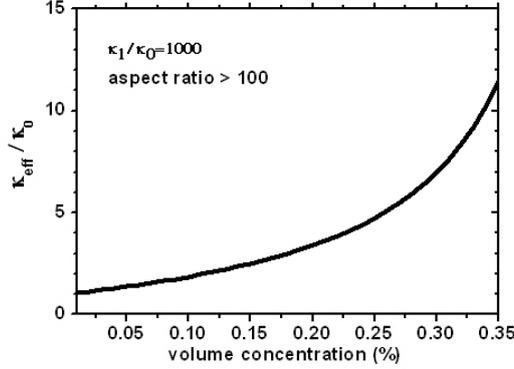
Fig. 2. Thermal conductivity enhancement of a matrix filled with graphene flakes of micrometer size calculated with the MGA model.

The graphene flakes are assumed micrometer-sized and randomly oriented. We observe a quite large thermal enhancement for relatively low volume concentration. This result suggests very low concentration threshold of percolation, which, as we mentioned before, cannot be assessed within MGA [29]. The enhancement factor induced by graphene flakes in the composite is about 12 for a volume concentration of 0.35%.

A more realistic model of graphene flakes would consider these flakes as disks of constant thickness (*i.e.*, flat) rather than an oblate spheroid. In a recent paper we have shown that for disks of constant thickness the depolarization factors along the graphene surface scales as follows: $1/2 - \chi_{x,y} \sim a_z/a_x$. For instance these depolarization factors would play a greater role for disks of constant thickness for aspect ratios $a_z/a_x \geq 1/100$. As a general rule the shape begins to matter when $(1/2 - \chi_k)k_1/k_0 > 1$. Numerical calculations of the eigenvalues χ_k and their weights w_k are performed with a method described in [22-25]. The results are presented in Table 1 for an aspect ratio $a_z/a_x = 1/10$. In parenthesis we have also displayed the eigenvalues and the corresponding weights of an oblate spheroid with the same aspect ratio.

Table 1. The most representative eigenmodes of a disk with an aspect ratio 1:10. Parallel as well as perpendicular field alignments are presented. In parenthesis we have shown the corresponding values of a similar oblate spheroid.

	χ_k	w_k		χ_k	w_k
	-0.34623	0.85882		0.409672	0.947441
	(-0.360804)	(1.0)		(0.430402)	(1.0)
	-0.196542	0.0601		0.199226	0.038049
Parallel	-0.143166	0.0014	Perpendicular	0.110443	0.0259643
	-0.101084	0.0154		-0.183744	0.0454102
	-0.058997	0.006			
	-0.0368618	0.0008			
	0.119884	0.063			

We can easily notice that the electrostatic operator of the flat disk has different spectral features than the electrostatic operator of the similar oblate spheroid. This issue may count when

a large thermal conductivity contrast is considered since the condition $(1/2 - \chi_k)k_1/k_0 > 1$ may be obeyed. Thus, the particle specific polarizations are different for these two shapes hence the effective thermal conductivity would be also different. Fig. 3 shows the calculations of the thermal conductivity of such nanocomposite made with fillers of graphene nanodots. The shape of the graphene nanodot is either a flat or an oblate disk. All calculations are performed within MGA. The black solid/dotted line is the effective conductivity of a composite with aligned flat/oblate disks. The red curves with symbols are for random orientation, namely the solid line denotes the effective thermal conductivity of a composite reinforced with flat disks and the dotted line denotes the effective thermal conductivity of a composite reinforced with oblate disks. Evidently, the thermal conductivity of composites reinforced with totally random flat disks is smaller than the conductivity of the composites reinforced with aligned flat disks.
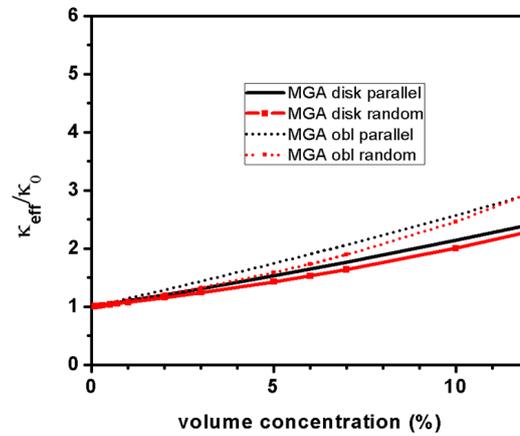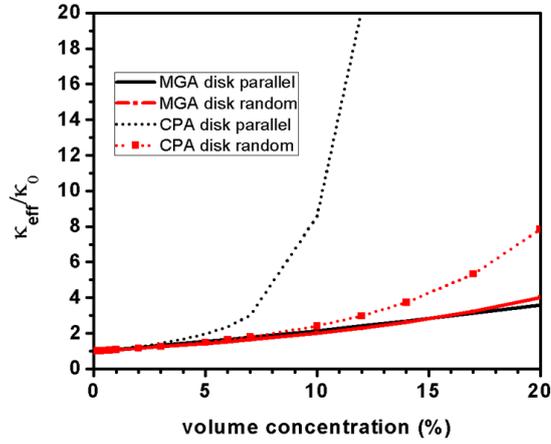

Fig. 3. Thermal conductivity enhancement of a matrix filled with graphene nanodots of about 5 nm wide (aspect ratio 1/10) calculated with MGA models of flat disk- and oblate-shaped fillers.

We further notice that the thermal effective conductivity of a nanocomposite reinforced with nanodots is smaller than that reinforced with larger flakes at the same volume concentration. Lastly and the most important, the oblate disk model of graphene nanodots overestimates the thermal conductivity enhancement with respect to the more realistic model of flat disks. This shape issue has been noticed not only for graphene nanodots [31] but also for carbon nanotubes [32] and it will be discussed elsewhere.

We also compared the results of MGA and CPA. These are depicted in Fig. 4 for flat nanodisks as fillers with an aspect ratio of 0.1. The black solid/dotted line is the effective conductivity of composites reinforced with aligned flat disks within MGA/CPA. The red curves with symbols are for random orientation of the fillers: the solid line indicates the effective conductivity within the Maxwell-Garnett approximation and the dotted line indicates the effective conductivity within the coherent potential approximation. As it can be seen from Fig. 4 in the low-concentration limit MGA and CPA give the same results. But the most important thing is the fact that CPA can catch the percolation phenomenon manifested by huge thermal enhancement. These calculations look pretty similar to those performed in [33], where an oblate model was used for graphene flakes. We calculated the percolation threshold for composites reinforced with aligned as well as with randomly oriented flat disks. Our calculations were fitted for $f > f_{th}$

to the equation $k_{eff} = k_1(f - f_{th})^\gamma$, where f_{th} is the percolation threshold concentration and γ is a percolation critical exponent. Thus, for composites reinforced with parallel oriented flat disks, we obtained $f_{th} = 10.86\%$ and $\gamma = 0.96$. In the same time, for composites reinforced with randomly oriented flat disks we obtained a larger percolation threshold concentration, $f_{th} = 14.83\%$, and a larger exponent, $\gamma = 1.79$. In contrast, the percolation threshold and the critical exponent for composites reinforced with oblate fillers with the same aspect ratio are $f_{th} = 8.14\%$ and $\gamma = 1.18$ [33]. As expected this value of the percolation threshold is smaller than the corresponding values obtained in the composite models reinforced with flat disks as fillers.

These calculations are performed assuming no interface thermal resistance and are valid also for electrical conductivity. The presence of interface thermal resistance reflects different physical mechanisms for thermal conductivity versus electrical conductivity [34]. Its effect is basically to downgrade the thermal contrast and to change the thermal percolation properties with respect to electrical ones [21].

Fig. 4. MGA versus CPA calculated thermal conductivity enhancement of a composite having flat disk-shaped graphene nanodots as inclusions of about 5 nm wide (aspect ratio 1/10).

4.   Conclusions

To conclude this work we have provided a practical method to calculate the effective thermal conductivity in composites having both arbitrarily shaped inclusions and interfacial thermal resistance in the Maxwell-Garnett approximation as well as in the coherent potential approximation. Graphene-based nanocomposites were analyzed with these techniques. Within Maxwell-Garnett approximation and without interface thermal resistance, our calculations show a thermal enhancement of 10–12 around 0.35% volume concentration of large graphene flakes at a thermal contrast of 1000 between the matrix and the inclusions. Also, in the Maxwell-Garnett approximation we have found that the oblate shape model of graphene nanodot fillers overestimates the effective thermal conductivity with respect to the flat disk model of the fillers. Finally, the coherent potential approximation is able to predict percolation threshold of composites reinforced by graphene nanodots.

References

[1] CHEN H., GINZBURG V. V., YANG J., YANG Y., LIU W., HUANG Y., DU L., CHEN B., *Thermal conductivity of polymer-based composites: Fundamentals and applications*, Progress in Polymer Science, **59**, pp. 41–85, 2016.

[2] NAN C.W, *Physics of inhomogeneous inorganic materials,* Prog. Mater. Sci., **37**, pp. 1–116, 1993.

[3] MINNICH A., CHEN, G., *Modified effective medium formulation for the thermal conductivity of nanocomposites*. Appl. Phys. Lett. **91**, pp. 073105–073107, 2007.

[4] JENG M.S., YANG R.G., SONG D., CHEN G., *Modeling the thermal conductivity and phonon transport in nanoparticle composites using Monte Carlo simulation.*, J. Heat Trans. Trans. ASME **130**, pp. 042410–042420, 2008.

[5] BALADIN A. A., *Thermal properties of graphene and nanostructured carbon materials*, Nat. Mater., **10**, pp. 569–581, 2011.

[6] SONG W. L., *et al.*, *Polymer/carbon nano-composites for enhanced thermal transport propertiescarbon nanotubes versus graphene sheets as nanoscale fillers*, J. Mater. Chem., **22**, pp. 17133–17140, 2012.

[7] SHAHIL K. M. F., BALADIN A. A., *Graphene –ultilayer Graphene Nanocomposites as Highly Efficient Thermal Interface Materials*, Nano Lett., **12**, pp. 861–867, 2012.

[8] LI A., ZHANG C., ZHANG Y. F., *Thermal Conductivity of Graphene-Polymer Composites: Mechanisms, Properties, and Applications*, Polymers, **9**, pp. 437–17, 2017.

[9] TORQUATO S., *Random Heterogeneous Materials: Microstructure and Macroscopic Properties*, Springer-Verlag, 2001.

[10] BROSSEAU C., BEROUAL A., *Computational electromagnetics and the rational design of new dielectric heterostructures*, Prog. Mater. Sci., **48**, pp. 373–456, 2003.

[11] MYROSHNYCHENKO V., BROSSEAU C., *Finite-element modeling method for the prediction of the complex effective permittivity of two-phase random statistically isotropic heterostructures*, J. Appl. Phys., **97**, pp. 044101–09, 2005.

[12] MAXWELL-GARNETT J. C., *Colours in Metal Glasses and in Metallic Films*, Philos Trans Royal Soc London, **203**, pp. 385–420, 1904.

[13] YONEZAWA F., MORIGAKI K, *Coherent Potential Approximation. Basic concepts and applications*, Prog. Theor. Phy. Suppl., **53**, pp, 1–76, 1973.

[14] SANDU T., KIRK W. P., *Generalized band anticrossing model for highly mismatched semiconductors applied to $BeSe_xTe_{1-x}$*, Phys. Rev. B, **72**, pp. 073204–4, 2005.

[15] SANDU T., KIRK W. P., *Electronic and optical properties of beryllium chalcogenide/silicon heterostructures*, Phys. Rev. B, **73**, pp. 235307–5, 2006.

[16] PLUGARU R., SANDU T., PLUGARU N., *First principles study and variable range hopping conductivity in disordered Al/Ti/Mn-doped ZnO*, Results in Physics, **2**, pp. 190–197, 2012.

[17] GUBERNATIS G. E., *Scattering theory and effective medium approximations to heterogeneous materials*, AIP Conf. Proc. **40**, pp. 84–98, 1978.

[18] ESHELBY J. D., *The determination of the elastic field of an ellipsoidal inclusion and related problems*, Proc. Roy. Soc. London A, **241**, pp. 376–385, 1957.

[19] HATTA H., TAYA M., *Equivalent Inclusion Method for Steady State Heat Conduction in Composites*, Int. J. Engng. Sci., **24**, pp. 1159–1172, 1986.

[20] NAN C. W., BIRRINGER R., CLARKE D. R., GLEITER H., *Effective thermal conductivity of particulate composites with interfacial thermal resistance*, J. Appl. Phys., **81**, pp. 6692–6699, 1997.

[21] SHTEIN M., NADIV R., BUZAGLO M., KAHIL K., REGEV O., *Thermally Conductive Graphene-Polymer Composites: Size, Percolation, and Synergy Effects*, Chem. Mater., **27**, pp. 2100–2106, 2015.

[22] SANDU T., VRINCEANU D., GHEORGHIU E., *Linear dielectric response of clustered living cells*, Phys. Rev. E, **81**, pp. 021913–11, 2010.

[23] SANDU T., VRINCEANU D., GHEORGHIU E., *Surface plasmon resonances of clustered nanoparticles*, Plasmonics, **6**, pp. 407–412, 2011.

[24] SANDU T., *Eigenmode decomposition of the near-field enhancement in localized surface plasmon resonances of metallic nanoparticles*, Plasmonics, **8**, pp. 391–402, 2013.

[25] SANDU T., BOLDEIU G., MOAGAR-POLADIAN V., *Applications of electrostatic capacitance and charging*, J. Appl. Phys. **114**, pp. 224904–10, 2013.

[26] SANDU T., BOLDEIU G., VOICU R., GOLOGANU M., *Modeling thermal conductivity of graphene-based nanocomposites*, 40th IEEE International Semiconductor Conference – CAS 2017, Sinaia, Romania, Proceedings, pp. 209–212, 2017.

[27] SIHVOLA A., KONG J. A., *Effective Permittivity of Dielectric Mixtures*, Trans. Geosci. Remote Sens. **26**, pp. 420–439, 1988.

[28] BRUGGEMAN D. A. G., Berechnung verschiedener physikalischer Konstanten von heterogenen Substanzen. I. Dielektrizittskonstanten und Leitfhigkeiten der Mischkrper aus isotropen Substanzen, Ann. Phys. (Leipzig), **24**, pp. 636–679, 1935.

[29] SIHVOLA A., SAASTOMOINEN S., HEISKA K., *Mixing Rules and Percolation, Remote Sensing Rev.*, **9**, pp. 39–50, 1994.

[30] VOICU R. C., SANDU T., *Analytical results regarding electrostatic resonances of surface phonon/plasmon polaritons: separation of variables with a twist*, Proc. R. Soc. A, **473**, pp. 2016079–9, 2017.

[31] SANDU T., TIBEICA C., VOICU R. C., *A heuristic look at plasmon resonances in graphene nanodisks*, 39th IEEE International Semiconductor Conference – CAS 2016, Sinaia, Romania, 2016, Proceedings, pp. 105–108, 2016.

[32] SANDU T., *Near-Field and Extinction Spectra of Rod-Shaped Nanoantenna Dimers*, Proceedings of the Romanian Acedemy, A, **15**, pp. 338–345, 2014.

[33] XIE S. H., LIU Y. Y., LI J. Y., *Comparison of the effective conductivity between composites reinforced by graphene nanosheets and carbon nanotubes*, Appl. Phys. Lett., **92**, 243121–3, 2008.

[34] NIKA D. L., POKATILOV E. P., ASKEROV A. S., BALADIN A. A., *Phonon thermal conduction in graphene: Role of Umklapp and edge roughness scattering*, Phys. Rev. B, **79**, pp. 155413–12, 2009.